Estimating spatial and temporal variations in solar radiation within Bordeaux winegrowing region using remotely sensed data

Benjamin Bois, Lucien Wald, Philippe Pieri, Cornelis van Leeuwen, Loïc Commagnac, Philippe Chery, Maxime Christen, Jean-Pierre Gaudillère, Etienne Saur

Bois B., Wald L., Pieri P., Van Leeuwen C., Commagnac L., Chery Ph., Christen M., Gaudillère J.-P., Saur E., Estimating spatial and temporal variations in solar radiation within bordeaux winegrowing region using remotely sensed data. *Journal International des Sciences de la Vigne et du Vin*, 42, 15-25, 2008.

ESTIMATING SPATIAL AND TEMPORAL VARIATIONS IN SOLAR RADIATION WITHIN BORDEAUX WINEGROWING REGION USING REMOTELY SENSED DATA

Benjamin Bois[a*], Lucien Wald[b] , Philippe Pieri[a] , Cornelis Van Leeuwen[ac] , Loic Commagnac[c] , Philippe Chery[c] , Maxime Christen[c] , Jean-Pierre Gaudillere[a] , Etienne Saur[cd]

[a]UMR EGFV, ISVV, INRA, Université Bordeaux 2, BP 81, 33883 Villenave d'Ornon Cedex, France

[b]CEP, Ecole de Mines de Paris, BP 207, F-06904 Sophia Antipolis Cedex, France

[c]Ecole Nationale d'Ingénieurs des Travaux Agricoles de Bordeaux, 1 cours du Général de Gaulle, 33175 Gradignan Cedex, France

[d]UMR TCEM, INRA, Université Bordeaux 1, BP 81, 33883 Villenave d'Ornon Cedex, France

**Corresponding author: Tel: 0033 557 122 501; Fax: 0033 557 122 515; email: benjaminbois@yahoo.fr*

***Abstract*:**

Aims: This paper presents a study solar radiation spatial and temporal variations in Bordeaux winegrowing area, for a 20 year period (1986-2005).

Methods and results: Solar radiation data was retrieved from the HelioClim-1 database, elaborated from Meteosat satellite images, using the Heliosat-2 algorithm. Daily data was interpolated using ordinary kriging to produce horizontal solar radiation maps at a 500 m resolution. Using a digital elevation model, high resolution daily solar radiation maps with terrain integration were then produced for the period 2001-2005, at a 50 m resolution. The long term (20 years) analysis of solar radiation at low spatial resolution (500 m) showed a west to east decreasing gradient within Bordeaux vineyards. Mean August-to-September daily irradiation values, on horizontal surface, were used to classify Bordeaux winegrowing areas in three zones: low, medium, and high solar radiation areas. This initial zoning was upscaled at 50 m resolution, applying a local correction ratio, based on 2001-2005 solar radiation on inclined surface analysis. Grapevine development and maturation potential of the different zones of appellation of origin of Bordeaux winegrowing area are discussed in relation with this zoning.

Conclusions: Solar radiation variability within Bordeaux winegrowing area is mainly governed by terrain slopes and orientations, which induce considerable variations within the eastern part of Bordeaux vineyards.

Significance and impact of the study: Solar radiation has a major impact on vineyard water balance, grapevine development and berry ripening. However, irradiation data is seldom available in weather stations records. This paper underline the interest of high resolution cartography of solar radiation, using satellite sensing and terrain effect integration, for agroclimatic studies in viticulture.

Keywords: *Solar radiation, remote sensing, Vitis vinifera, cartography, Bordeaux vineyards.*

1 INTRODUCTION

Solar radiation has a large influence on vine growth, berry ripening, and disease development in vineyards. Its effects are numerous, and it affects other climate variables. Hence, vineyard microclimate depends strongly on this variable. Most of the radiative balance is determined by incoming solar radiation. It induces variations of surface and air temperature, and it has a major role in evaporative processes, such as evapotranspiration (Priestley and Taylor, 1972; Bois et al., 2005). Solar radiation determines incoming light and photosynthetically active radiations (PAR). For grapevine (*Vitis vinifera L.*), as for most of the plants, light availability increases dry mass production (Buttrose, 1969; Grechi et al., 2007). But in hot and dry conditions, photosynthesis can be reduced despite non limiting light conditions (Zufferey et al., 2000). Several researches have enlightened the difficulties to separate temperature from light effects on photosynthesis activity and berry maturation in natural conditions, as incoming solar radiation determines both of these climatic variables (Crippen and Morrison, 1986; Schultz et al., 1996; Bergqvist et al., 2001). Results concerning the influence of sun exposition on berries differ according to locations and experimental conditions. Overexposure to sunlight may decrease anthocyanin contents of berries (Bergqvist et al., 2001) and sugar concentration (Kliewer and Lider, 1968). However, sugar concentration level may increase in sun exposed berries due to water loss (Crippen and Morrison, 1986). In all experiments, sunlight-exposed fruits are lower in malate concentration and total titrable acidity (Kliewer and Lider, 1968; Kliewer, 1977; Crippen and Morrison, 1986 ; Dokoozlian and Kliewer, 1996; Spayd et al., 2002). Theses results, sometimes contradictory, highlight the fact that management of incoming solar radiation via vineyard architecture has to be adapted to local conditions (i.e. local climate and soil characteristics). Models have been developed to

integrate the quantity of solar irradiation intercepted by leaf area according to vineyard architecture, in order to estimate grapevine transpiration and vineyard soil water balance (Riou et al., 1989; Riou et al., 1994; Lebon et al., 2003; Oyarzun et al., 2007).

Solar radiation data is seldom available in weather records, for its precise measurement requires steadily maintained fragile devices, such as pyranometers. However,with recent advances in remote sensing and image analysis, it is now possible to retrieve daily solar radiation from satellite data (Solanki et al., 2005). The HelioClim-1 database, elaborated from Meteosat images analysis provides solar radiation data for Europe and Africa (Lefèvre et al., 2007). This database was used to establish the European Solar Radiation Atlas (ESRA, Rigollier et al., 2000), and was coupled to a 2 km resolution Digital Elevation Model (DEM) to include the effects of relief on solar radiation interception for photovoltaic potential cartography of Africa (Huld et al., 2005).

Orography has a major effect on incoming solar radiation, especially when close to equinox, between 30° and 60° latitudes (Oke, 1978). Advances in computer technology and development of GIS software allow to easily determine spatial variations of solar irradiation provided by terrain slope and aspect (Durand and Legros, 1981; Flint and Childs, 1987; Hofierka and Suri, 2002; Kang et al., 2002; Wang et al., 2002).

We propose here to combine satellite sensed data and solar irradiation models based upon orography to estimate spatial and temporal variability of solar radiation interception of Bordeaux winegrowing area, France. The results provided by the cartography methods are used as a tool for viticulture zoning.

2 MATERIAL AND METHODS

2.1 Study area

The winegrowing area of Bordeaux is located in Southwest of France, in the province (“*département”*) of Gironde. It is composed of 57 appellations of controlled origin (AOC) covering about 230 000 ha, although only 120 000 ha are actually planted with grapevine. Bordeaux vineyards are located at 20 to 150 kilometers from the Atlantic Ocean, between 45.5°N and 44.3°N (figure 1A and 1B). The Bordeaux vineyards can be divided in 5 sub-regions, as shown on figure 1B and in table 1.

The climate is temperate, with moderately dry summers (200 mm from July to September) and wet autumn and winter periods. The average annual rainfall is 930 mm (1976-2005 mean) and ranges from 700 to 1300 mm according to the year. The mean annual temperature is 13.8°C, and ranges from 22.3°C in August to 7.8°C in December. The large area of the

Bordeaux vineyards provides a considerable diversity of climatic conditions, due to several topographic elements: the Medoc region, (in the north of region I, figure 1B), is caught between the Atlantic Ocean and the Gironde Estuary. In South-East, the eastern Entre-Deux-Mers area is marked by frequent storms during summer. Most of the western side of the Bordeaux winegrowing area is flat, whereas the eastern part is hilly. Some of the vineyards are located within the suburbs of Bordeaux city and benefit from higher temperature, due to urban heat island effects (Oke, 1978).

Grapevine cultivars are mostly Merlot, Cabernet-Sauvignon, Cabernet franc for red varieties, and Sauvignon blanc and Semillion for white varieties.

2.2 Solar radiation cartography

2.2.1 Solar radiation on horizontal surfaces

Daily solar irradiation data was taken from the HelioClim-1 database, available at the SoDa Web Service (http://www.soda-is.org, Gschwind et al., 2006). This database has been obtained by the application of the Heliosat-2 method to reduced data sets ISCCP-B2 Meteosat satellite images (Lefèvre et al., 2007). The Heliosat-2 method is based upon the construction of *cloud* and *clear-sky indexes*, for each pixel of a satellite image (Rigollier et al., 2004). The precision of the method depends mostly on the cloud cover: relative uncertainties are lower during clear-sky days (Rigollier et al., 2004). The HelioClim-1 database provides root mean squared differences of about 20% of daily pyranometers values for Europe and Africa (Lefèvre et al., 2007). Heliosat-2 method does not account for slope and aspect of the terrain.

Daily solar irradiation data was collected for the period 1986-2005. Daily solar irradiation data was downloaded at 418 points, each sampled at an approximate distance of 20 kilometres inside and at neighbouring sites of Gironde.

From daily irradiation data, cloud cover temporal patterns were analyzed using a clearness index (K_T), calculated as follows:

$$K_T = \frac{G_{dh}}{G_{d0}} \qquad [1]$$

where G_{dh} is the daily irradiation on horizontal surface (in MJ m^{-2}), G_{d0} is the daily extra-atmospheric irradiation (in MJ m^{-2}). G_{d0} was calculated with astronomical formulae.

Mean daily irradiations on several periods and mean monthly K_T values were then interpolated on a 500 m resolution grid, using the ordinary kriging technique. A review on geostatistical techniques can be found in Goovaerts (1999). Kriging was done using the Gstat package of the R statistical software (Pebesma, 2004; R Development Core Team, 2007).

Linear co-variance models were fitted automatically to experimental semi-variograms, by least squared method.

2.2.2 Terrain integration for incoming solar radiation cartography

Effects of terrain on solar irradiation were taken into account by mean of direct geometrical relations. The solar radiation model *r.sun* (Hofierka and Suri, 2002), implemented in GRASS Geographical Information System (GIS) was used. The *r.sun* model estimates beam, diffuse and reflected components of solar incoming radiation on horizontal and inclined surfaces. Daily solar irradiation is calculated at a 15' time step and cumulated for each day. Mask effects of surrounding orography are taken into account.

Terrain effects on solar radiation interception are considerable during clear-sky days, as most of the incoming radiation is direct, and relationship between irradiation and orography is geometric. During cloudy days, most of the incoming radiation is diffuse. In such situations, except the mask effects produced by surrounding relief, terrain effects are minor. For oceanic climate conditions, such as Bordeaux area, cloudy days frequency is not negligible. For this reason, we used the *r.sun* model, which integrates diffuse radiation (standard overcast method).

Input data for *r.sun* are: elevation, slope and aspect (retrieved from a 50 m resolution Digital Elevation Model (DEM)); ground albedo (set to 0.2), horizontal surface irradiation from HelioClim-1 database; Linke turbidity coefficient, whose monthly values were provided by the SoDa Web service; diffuse (k_{dh}) and beam (k_{bh}) proportions (*i.e.* values from 0 to 1) of daily irradiation on horizontal surfaces, estimated with an empirical relationship established at Bordeaux (Pieri and Valancogne, personal communication) :

$$k_{dh} = \min\left(1.09 - 2.6896\left(\frac{G_{dh}}{G_{\mathrm{d0}}}\right)^2 + 1.2843\left(\frac{G_{dh}}{G_{\mathrm{d0}}}\right)^3 ; 1\right) \qquad [2]$$

and

$$k_{dh} = 1 \; if \; \left(\frac{G_{dh}}{G_{\mathrm{d0}}}\right) < 0.2 \qquad [3]$$

and

$$k_{bh} = 1 - k_{dh} \qquad [4]$$

where G_{dh} and G_{d0} have the same signification and units as in equation [1].

The *r.sun* model provided daily beam, diffuse and reflected solar radiation on inclined surfaces, at the DEM resolution (*i.e.* 50 m by 50 m). These three variables were then summed

to obtain daily irradiation data. The inter-annual differences between horizontal and inclined surfaces were evaluated on a 5 year period, from 2001 to 2005.

3 RESULTS

3.1 Solar radiation climatology in Bordeaux area

Annual mean of daily solar irradiation, annual sunshine duration and annual clear-sky frequency data of Gironde province and Bordeaux winegrowing area are shown in table 2. Mean daily irradiation ranges from 11.67 to 13.34 MJ m^{-2} (-5% to 9% of the mean value) for the Gironde province and from 11.67 to 12.83 MJ m^{-2} in Bordeaux winegrowing area (-3% to 7% of the mean value). The average clearness index is 0.44 for Gironde province and 0.433 for Bordeaux wine growing area. Solar irradiation reaches its maximum in June and July (figure 2). It remains low from October to February (mean daily irradiation below 10 MJ m^{-2}). The spatial variation of solar irradiation is larger for the Gironde province than for Bordeaux winegrowing area (figure 2).

The winegrowing season, spanning a period from April to September, benefits from clearness indices from 0.46 to 0.58 (figures 3A and 3B) in Gironde province. During the autumn period, the proportion of extra-atmospheric global radiation that reaches the ground is lower that during other seasons (figure 3C). This could be explained both by the cloud climatology (weather is globally cloudier from October to February in Gironde province) and the increasing length of solar radiation path throughout the atmosphere, due to sun inclination. The spatial patterns of clearness index remain similar throughout the year: the Atlantic Ocean coast receives the highest amount of solar radiation. The clearness index decreases from west to east, during spring, summer and winter. During autumn, it decreases from west to east until the center of Gironde province, and then increases again towards east (figure 3C). This particular spatial pattern might be related to the greater diversity of synoptic situations during this period (Jones and Davis, 2000). The largest spatial variability is observed during winter.

The western part of Bordeaux winegrowing area receives the highest amount of solar radiation. In Medoc, located in the north-west of Gironde (region I, see figure 1), clearness index is 4 to 8% higher than in the easternmost vineyards, from April to September (figures 3A and 3B).

3.2 Bordeaux vineyards zoning

In Bordeaux winegrowing area, veraison of red and white grape varieties generally occur at the end of July or at the beginning of August. The harvest period ranges from mid-September

to beginning of October. As climate conditions are crucial from veraison to harvest, mean daily values of solar irradiation from August to September on horizontal surface were calculated. This index is referred hereafter as $G_{mat,h}$ (where *mat* stands for maturation period, i.e. august to September, and *h* indicates that G_{mat} is calculated on a horizontal surface). It was used to perform a zoning of Bordeaux winegrowing area, as follows: (a) Mean $G_{mat,h}$ on a 20 year period was calculated for each pixel located in Bordeaux winegrowing area ; (b) all the pixel values were classified in 3 classes with regular interval. Classes obtained correspond to low, middle and high $G_{mat,h}$ values (table 3, figure 4B). The first class ("low") corresponds to a mean daily irradiation (for August and September) ranging from 15.36 to 15.84 MJ m^{-2}, with a mean value of 15.68 MJ m^{-2}. For the second class ("medium"), $G_{mat,h}$ ranges from 15.85 to 16.33 MJ m^{-2}, with a mean value of 16.03 MJ m^{-2}. For the third class ("high"), $G_{mat,h}$ ranges from 16.33 to 16.81 MJ m^{-2}, with a mean value of 16.48 MJ m^{-2}. Whereas the total amplitude of $G_{mat,h}$ observed within the Bordeaux winegrowing equals 8.9% of the mean horizontal value, the difference between the mean values are small (-2.2% between low and medium, and 2.8% between medium and high). Class 1 (low $G_{mat,h}$ value) represent 66% of the total area of Bordeaux vineyards, class 2 (medium) 32% and class 3 (high) 2%.

The western and the southern parts of Bordeaux winegrowing area (region I and II, and the west of region V) are located in the medium $G_{mat,h}$ value zone, and eastern part of Bordeaux winegrowing area (region III and IV) is located in the low $G_{mat,h}$ value zone, as well as the eastern part of region V (figure 4A). A small area, the northwesternmost part of Bordeaux vineyards (region I) is located in high $G_{mat,h}$ value zone.

3.3 Terrain integration on solar radiation zoning

Solar daily irradiation data with terrain effects integration was calculated for the period 2001-2005, using the *r.sun* algorithm, at the DEM cell resolution, i.e. a 50 m by 50 m pixel. This high resolution cartography has a high computational cost: it is both time and hard-disk-space consuming, and the calculation on a 20 years period would have taken several weeks of computer calculations. To reduce computational cost, G_{mat} (i.e. mean daily irradiation from August to September, with terrain effects integration) for the 20 year period was obtained using an empirical correction factor calculated for the period 2001-2005: G_{mat} for the 20 years period was assessed by multiplying $G_{mat,h}$ (1986-2005) by the 5 years average (2001-2005) of the ratio $G_{mat\ h}/G_{mat}$ calculated for each 50 m pixel. We assumed that, for each 50 m pixel, having its own terrain characteristics (i.e. slope inclination and aspect), the ratio between G_{mat} (computed using daily irradiation data with terrain integration, at high resolution) and $G_{mat,h}$

(horizontal irradiation data, at 500 m resolution) remained constant. This was verified with the 2001-2005 high resolution data set: The relative difference for each pixel (i.e. (G_{mat} − $G_{mat,h}$)/ $G_{mat,h}$) is almost the same from 2001 to 2005 (figure 5). In other words, the effect of terrain on solar radiation interception during August and September is quasi-identical from one year to another.

A new zoning was achieved, using the high resolution G_{mat} on the period 1986-2005 to classify Bordeaux winegrowing area in the 3 classes ("low", "medium" and "high") previously obtained with $G_{mat,h}$. The repartition of Bordeaux's appellations of origin before and after the integration of terrain effects on solar radiation interception is shown in table 4. In the region I, the zoning changes for three appellations of origin areas: 16 to 36% of Listrac, Médoc and Moulis appellations total areas are situated in high G_{mat} class after terrain integration, whereas they were located in medium class in flat terrain zoning. The $G_{mat,h}$ values of these areas are close to the threshold values of medium-high classes, which explains that a small variation in incoming solar radiation induced by terrain modified strongly the zoning. For regions II, III, IV and V, the classification was considerably modified. For example, 93% of Entre-Deux-Mers appellation of origin was classified in low $G_{mat,h}$ zone. With terrain integration, 63% of the area remains in low G_{mat} zone, one third is classified in medium G_{mat} zone, and 4% of the area is classified in high G_{mat} zone. The well-known area of Saint-Emilion, as well, receives little solar radiation during August and September, compared to the whole Bordeaux winegrowing area. 100% of the total surface area of this appellation was located in low $G_{mat,h}$ area, when considering incoming radiation on horizontal surface. With terrain effects integration, 8% of the appellation changes of class: 6% of the appellation is classified as a medium G_{mat} area, and 2% as high G_{mat} area. Figure 6B shows that the south-exposed slopes close to Saint-Emilion village receive from 1 to 10% more solar radiation than the mean value of the area.

Another example is the appellation of origin Côtes-de-Bourg, where 48% of the area is classified in a low $G_{mat,h}$ area and 52% of the total area is classified in a medium $G_{mat,h}$ area. After terrain integration, 12% of the total area is situated in low G_{mat} class. G_{mat} within the appellation of origin Côtes de Bourg varies from -14% to +13% of the mean appellation value (figure 6A).

4 DISCUSSION AND CONCLUSIONS

Satellite sensed solar radiation, from the HelioClim-1 database, combined with terrain information was used to calculate solar irradiation for the large wine growing area, at a high

resolution (50m). The studied period (1985-2005) is sufficiently long to provide a robust analysis of solar radiation climatology of Bordeaux vineyards. Such study would not have been possible using ground measurement devices, such as pyranometers. Firstly, because pyranometer devices are quite recent and the technology has been improved, so data would have required several recalibration. Secondly, only a small number of weather stations located close to or within Bordeaux vineyards provide solar radiation records, for such a long period (less than 5 stations). However, our high resolution spatialized solar irradiation daily values (50 m) underestimate solar radiation. They have been compared to pyranometer records of the weather station of Villenave d'Ornon (located between regions I and II), for the period 2001-2005. They showed a mean difference (bias) of -1.5 MJ m^{-2}, indicating a underestimation of 11.1% of the annual mean (table 5). The root mean squared difference was 2.7 MJ m^{-2} (19.8% of the mean annuel pyranometer value). For G_{mat}, the bias and root mean squared differences are -9.8% and 16.6% of the annual mean, respectively. These errors stay in the range of uncertainties provided by the use of pyranometer measurements (Llasat and Snyder, 1998; Droogers and Allen, 2002). Although the relative spatial differences presented in this study have not been affected by this underestimation, the absolute values may be slightly higher.

It has been shown that the western part of Bordeaux vineyards receive more solar radiation than the eastern part, throughout the year. As the ripening of grapevine varieties of Bordeaux area occurs during the August and September, a zoning based on the mean daily irradiation during this period (referred as $G_{mat,h}$) was proposed. The Bordeaux winegrowing area was partitioned into three classes: low, medium and high $G_{mat,h}$ values. The southern and the eastern parts of Bordeaux winegrowing region receive the highest amount of solar radiation during berry ripening period. When increasing the resolution of the zoning, using the *r.sun* model, it has been shown that terrain effects on solar radiation are not negligible, although the Bordeaux winegrowing area could not be considered as a mountainous region. Well exposed (south) slopes of the eastern part of Bordeaux vineyards receive as much solar radiation as flat surfaces in the western part. Failla *et al*. (2004) have found that slopes that receive a higher amount of solar radiation were associated with earlier phenology, higher sugar content, lower titrable acidity and lower phenolic content in berries, in red cv. Nebbiolo vineyards.

The attempt of the present work was to evaluate solar radiation climatology of Bordeaux winegrowing area, and to propose a new zoning approach for ripening potential of vineyards. The assumptions made prior to such zoning are multiple: firstly, solar irradiation affects berry ripening (Dokoozlian and Kliewer, 1996; Bergqvist et al., 2001). Secondly, solar irradiation has a major effect on surface and air temperature, which affect grapevine phenology, malate

degradation within berries, polyphenolic, sugar and aromatic contents of berries (Buttrose et al., 1971; Reynolds and Wardle, 1989; Bergqvist et al., 2001; Spayd et al., 2002). Thirdly, as spatial variation of cumulated incoming solar radiation during berry maturation period depends mainly on vineyard slopes and aspects, it is associated with different water runoff patterns, due to slope intensity. It can be expected that steep slopes will be associated with higher runoff. Finally, solar radiation plays a major role in vineyard transpiration and it is a key parameter of water balance models (Trambouze and Voltz, 2001; Lebon et al., 2003). Hence, south-exposed vineyards would certainly be subject to higher evaporative demands. Increasing G_{mat} index may thus be associated to higher water deficits.

Row orientations and spacing, as well as canopy structure dramatically affect incoming solar radiation distribution between grapevine rows and bare or grass-covered surface (Smart, 1973; Pieri and Gaudillere, 2003, 2005). Oyarzun et al. (2007) recently proposed a solar radiation interception model for horizontal and inclined surface in orchards and vineyards. Coupling this kind of model to satellite sensed solar radiation, water runoff and water balance models would certainly improve general knowledge about inclined surface effects on grapevine development and berry maturation.

Acknowledgements **:** The authors thank the Conseil Interprofessionnel des Vins de Bordeaux for their technical and financial support.

REFERENCES

Bergqvist, J., Dokoozlian, N. and Ebisuda, N. (2001). Sunlight exposure and temperature effects on berry growth and composition of Cabernet-Sauvignon and Grenache in the Central San Joaquin Valley of California. American Journal of Enology and Viticulture, 52(1):1-7.

Bois, B., Pieri, P., Leeuwen, C.v. and Gaudillere, J.P., 2005. Sensitivity analysis of the Penman-Monteith evapotranspiration formula and comparison of empirical methods used in viticulture soil water balance, XIV International GESCO Viticulture Congress, Geisenheim, Germany, 23-27 August, 2005.

Buttrose, M.S. (1969). Vegetative growth of grapevine varieties under controlled temperature and light intensity. Vitis, 8: 280-285.

Buttrose, M.S., Hale, C.R. and Kliewer, W.M., 1971. Effect of the temperature on the composition of Cabernet-Sauvignon berries. American Journal of Enology and Viticulture, 22(2): 71-75.

Crippen, D.D., Jr. and Morrison, J.C. (1986). The effects of sun exposure on the compositional development of Cabernet Sauvignon berries. American Journal of Enology and Viticulture, 37(4): 235-242.

Dokoozlian, N.K. and Kliewer, W.M. (1996). Influence of light on grape berry growth and composition varies during fruit development. Journal of the American Society for Horticultural Science, 121(5): 869-874.

Droogers, P. and Allen, R.G., 2002. Estimating reference evapotranspiration under inaccurate data conditions. Irrigation and Drainage Systems, 16(1): 33-45.

Durand, R. and Legros, J.P. (1981). Cartographie automatique de l'energie solaire en fonction du relief. Agronomie, 1(1): 31-39.

Failla, O., Mariani, L., Brancadoro, L., Minelli, R., Scienza, A., Murada, G., Mancini, S.., 2004. Spatial distribution of solar radiation and its effects on vine phenology and grape ripening in an alpine environment. American Journal of Enology and Viticulture, 55(2): 128-138.

Flint, A.L. and Childs, S.W. (1987). Calculation of solar radiation in mountainous terrain. Agricultural and Forest Meteorology, 40(3): 233-249.

Goovaerts, P., 1999. Geostatistics in soil science: state-of-the-art and perspectives. Geoderma, 89(1-2): 1-45.

Grechi, I., Vivin, P., Hilbert, G., Milin, S., Robert, T., Gaudillere, J.-P. (2007). Effect of light and nitrogen supply on internal C:N balance and control of root-to-shoot biomass allocation in grapevine. Environmental and Experimental Botany, 59(2): 139-149.

Gschwind, B., Menard, L., Albuisson, M. and Wald, L., 2006. Converting a successful research project into a sustainable service: The case of the SoDa Web service. Environmental Modelling & Software, 21(11): 1555-1561.

Hofierka, J. and Suri, M., 2002. The solar radiation model for Open source GIS: implementation and applications., Open source GIS - GRASS users conference 2002, Trento, Italy.

Huld, T., Suri, M., Dunlop, E. and Wald, L., 2005. Integration of Helioclim-1 database into PV-GIS to estimate solar electricity potential in Africa, 20th European Photovoltaic Solar Energy Conference and Exhibition, Bacelona, Spain.

Jones, G.V. and Davis, R.E., 2000. Using a synoptic climatological approach to understand climate-viticulture relationships. International Journal of Climatology, 20(8): 813-837.

Kang, S., Kim, S. and Lee, D. (2002). Spatial and temporal patterns of solar radiation based on topography and air temperature. Canadian Journal of Forest Research, 32(3): 487-497.

Kliewer, W.M. (1977). Influence of temperature, solar radiation and nitrogen on coloration and composition of Emperor grapes. American Journal of Enology and Viticulture, 28(2): 96-103.

Kliewer, W.M. and Lider, L.A. (1968). Influence of cluster exposure to the sun on the composition of thompson seedless fruit. American Journal of Enology and Viticulture, 19(3): 175-184.

Lebon, E., Dumas, V., Pieri, P. and Schultz, H.R. (2003). Modelling the seasonal dynamics of the soil water balance of vineyards. Functional Plant Biology, 30(6): 699-710.

Lefèvre, M., Wald, L. and Diabate, L. (2007). Using reduced data sets ISCCP-B2 from the Meteosat satellites to assess surface solar irradiance. Solar Energy, 81(2): 240-253.

Llasat, M.C. and Snyder, R.L., 1998. Data error effects on net radiation and evapotranspiration estimation. Agricultural and Forest Meteorology, 91(3/4): 209-221.

Oyarzun, R.A., Stockle, C.O. and Whiting, M.D. (2007). A simple approach to modeling radiation interception by fruit-tree orchards. Agricultural and Forest Meteorology, 142(1): 12-24.

Pebesma, E.J., 2004. Multivariable geostatistics in S: the gstat package. Computers & Geosciences, 30(7): 683-691.

Pieri, P. and Gaudillere, J.P., 2003. Sensitivity to training system parameters and soil surface albedo of solar radiation intercepted by vine rows. Vitis, 42(2): 77-82.

Pieri, P. and Gaudillere, J.P., 2005. Vines water stress derived from a soil water balance model - sensitivity to soil and training system parameters, XIV International GESCO Viticulture Congress, Geisenheim, Germany, 23-27 August, 2005, 457-463.

Priestley, C.H.B. and Taylor, R.J., 1972. On assessment of surface heat flux and evaporation using large-scale parameters. Monthly Weather Review, 100(2): 81-92.

R Development Core Team, 2007. R: A Language and Environment for Statistical Computing. R Foundation for Statistical Computing, Vienna, Austria.

Reynolds, A.G. and Wardle, D.A., 1989. Influence of fruit microclimate on monoterpene levels of Gewurztraminer. American Journal of Enology and Viticulture, 40(3): 149-154.

Rigollier, C., Bauer, O. and Wald, L., 2000. On the clear-sky model of the ESRA - European Solar Radiation Atlas - with respect to the Heliosat method. Solar Energy, 68(1): 33-48.

Rigollier, C., Lefèvre, M. and Wald, L. (2004). The method Heliosat-2 for deriving shortwave solar radiation from satellite images. Solar Energy, 77(2): 159-169.

Riou, C., Pieri, P. and Clech, B.l., 1994. Water use of grapevines well supplied with water. Simplified expression of transpiration. Vitis, 33(3): 109-115.

Riou, C., Valancogne, C. and Pieri, P., 1989. Un modèle simple d'interception du rayonnement solaire par la vigne. Vérification expérimentale. Agronomie, 9(5): 441-450.

Schultz, H.R., Kiefer, W. and Gruppe, W., 1996. Photosynthetic duration, carboxylation efficiency and stomatal limitation of sun and shade leaves of different ages in field-grown grapevine (Vitis vinifera L.). Vitis, 35(4): 169-176.

Smart, R.E. (1973). Sunlight interception by vineyards. American Journal of Enology and Viticulture, 24 (4): 141-147.

Solanki, S.K., Krivova, N.A. and Wenzler, T., 2005. Irradiance models. Advances in Space Research, 35: 376-383.

Spayd, S.E., Tarara, J.M., Mee, D.L. and Ferguson, J.C. (2002). Separation of sunlight and temperature effects on the composition of Vitis vinifera cv. Merlot berries. American Journal of Enology and Viticulture, 53(3): 171-182.

Trambouze, W. and Voltz, M. (2001). Measurement and modelling of the transpiration of a Mediterranean vineyard. Agricultural and Forest Meteorology, 107(2): 153-166.

Turc, L., 1961. Evaluation des besoins en eau d'irrigation, évapotranspiration potentielle. Annales Agronomiques, 12(1): 13-49.

Wang, S., Chen, W. and Cihlar, J. (2002). New calculation methods of diurnal distribution of solar radiation and its interception by canopy over complex terrain. Ecological Modelling, 155(2/3): 191-204.

Wei, C.-P., Lee, Y.-H. and Hsu, C.-M., 2003. Empirical comparison of fast partitioning-based clustering algorithms for large data sets. Expert Systems with Applications, 24(4): 351-363.

Zufferey, V., Murisier, F. and Schultz, H.R., 2000. A model analysis of the photosynthetic response of Vitis vinifera L. cvs Riesling and Chasselas leaves in the field: I. Interaction of age, light and temperature. Vitis, 39(1): 19-26.

Table 1: Classification by region of appellations of origin of Bordeaux winegrowing area (see figure 2)

Region	Appellations of origin (AOC)
I	Bordeaux ; Bordeaux Supérieur ; Haut-Médoc ; Listrac ; Margaux ; Médoc ; Moulis ; Pauillac ; Saint-Estèphe ; Saint-Julien
II	Barsac ; Bordeaux ; Bordeaux Supérieur ; Cerons ; Graves ; Graves Supérieures ; Pessac-Léognan ; Sauternes
III	Bordeaux ; Bordeaux Supérieur ; Côtes de Bordeaux ; Saint-Macaire ; Entre-Deux-Mers ; Haut-Bénauge ; Graves-de-Vayres ; Loupiac ; Premières Côtes de Bordeaux ; Cadillac ; Sainte-Croix-du-Mont ; Sainte-Foy Bordeaux
IV	Bordeaux ; Bordeaux Supérieur ; Côtes de Francs ; Côtes de Castillon ; Lalande de Pomerol ; Lussac Saint-Emilion ; Montagne Saint-Emilion ; Pomerol ; Puisseguin Saint-Emilion ; Saint-Emilion ; Saint-Georges Saint-Emilion
V	Blaye ; Blayais ; Bordeaux ; Bordeaux Supérieur ; Canon Fronsac ; Côtes de Bourg ; Fronsac ; Premières Côtes de Blaye ; Côtes de Blaye

Table 2: Spatial variations statistics of solar radiation climatological data, on the period 1986-2005, for Gironde province and Bordeaux vineyards. CV = coefficient of variation (mean divided by the standard deviation, σ).

	Gironde Province		**Bordeaux vineyards**	
	Daily irradiation (Wh m-2)	**Clearness index (K_T)**	**Daily irradiation (Wh m-2)**	**Clearness index (K_T)**
Min.	11.7	0.42	11.7	0.425
1st quartile	12.0	0.43	11.8	0.428
Median	12.2	0.44	11.9	0.431
Mean	12.3	0.44	12.0	0.433
3rd quartile	12.5	0.45	12.0	0.435
Max.	13.3	0.48	12.8	0.463
σ	0.38	0.01	0.20	0.007
CV	3.1%	2.9%	1.7%	1.6%

Table 3: Statistics of mean solar irradiation (MJ m^{-2}) from August to September, for three classes obtained by regular interval clustering, in Bordeaux winegrowing area. CV = coefficient of variation (the mean divided by the standard deviation, σ).

	Horizontal surface classes			**Inclined surface classes**		
	Low	**Medium**	**High**	**Low**	**Medium**	**High**
Mean	15.68	16.03	16.48	15.59	16.05	16.50
σ	0.10	0.15	0.14	0.22	0.14	0.18
CV	0.6%	0.9%	0.8%	1.4%	0.9%	1.1%
Min.	15.36	15.85	16.33	12.38	15.85	16.33
Max.	15.84	16.33	16.81	15.85	16.33	17.80
Area (ha.)	156106	77065	3889	127819	92962	16279

Table 4: Distribution of appellation of origin areas, within the three solar radiation zones (i.e. classes), before and after integration of terrain.

Region	Appellation of origin (A.O.C.)	Horizontal surface G_{mat} zones[a]			G_{mat} zones with terrain effects integration[a]			Total area (ha)
		Low	Medium	High	Low	Medium	High	
I	**Bordeaux ; Bordeaux supérieur**	-	99%	1%	-	99%	1%	**1472**
	Haut-Médoc	-	97%	3%	-	81%	19%	**9077**
	Listrac	-	73%	27%	-	48%	52%	**1393**
	Margaux	-	100%	-	-	94%	6%	**1856**
	Médoc	-	70%	30%	-	54%	46%	**10419**
	Moulis	-	94%	6%	-	60%	40%	**1034**
	Pauillac	-	100%	-	2%	96%	2%	**1600**
	Saint-Estèphe	-	100%	-	-	92%	8%	**1552**
	Saint-Julien	-	100%	-	-	94%	6%	**997**
II	**Barsac**	-	100%	-	4%	96%	-	**860**
	Bordeaux ; Bordeaux supérieur	-	100%	-	15%	83%	2%	**3131**
	Cerons ; Graves ; Graves supérieures	-	100%	-	10%	89%	1%	**2446**
	Graves ; Graves supérieures	-	100%	-	20%	78%	2%	**8994**
	Pessac-Léognan	-	100%	-	13%	85%	2%	**4514**
	Sauternes	-	100%	-	22%	75%	3%	**2154**
III	**Bordeaux ; Bordeaux supérieur**	69%	31%	-	69%	30%	1%	**4471**
	Côtes de Bordeaux ; Saint-Macaire	25%	75%	-	39%	47%	14%	**4498**
	Entre-Deux-Mers	93%	7%	-	63%	33%	4%	**59325**
	Entre-Deux-Mers ; Bordeaux ; Haut-Benauge	99%	1%	-	48%	47%	5%	**6809**
	Graves de Vayres	100%	-	-	89%	11%	-	**1370**
	Loupiac	-	100%	-	45%	40%	15%	**828**
	Premières Côtes de Bordeaux	88%	12%	-	60%	33%	7%	**4207**
	Premières Côtes de Bordeaux ; Cadillac	42%	58%	-	40%	40%	20%	**8356**
	Sainte-Croix-Du-Mont	-	100%	-	33%	31%	36%	**760**
	Sainte-Foy Bordeaux	100%	-	-	79%	20%	1%	**16425**
IV	**Bordeaux ; Bordeaux supérieur**	100%	-	-	97%	3%	-	**7379**
	Bordeaux ; Côtes de Francs	100%	-	-	86%	14%	-	**1030**
	Côtes de Castillon	100%	-	-	80%	17%	3%	**5608**
	Lalande de Pomerol	100%	-	-	96%	4%	-	**1378**
	Lussac Saint-Emilion	100%	-	-	90%	9%	1%	**1834**
	Montagne Saint-Emilion	100%	-	-	83%	16%	1%	**2097**
	Pomerol	100%	-	-	100%	-	-	**978**
	Puisseguin Saint-Emilion	100%	-	-	84%	14%	2%	**1041**
	Saint-Emilion	100%	-	-	92%	6%	2%	**7153**
	Saint-Georges Saint-Emilion	100%	-	-	61%	38%	1%	**274**
V	**Blaye ; Blayais**	66%	34%	-	59%	41%	-	**2426**
	Bordeaux ; Bordeaux supérieur	98%	2%	-	83%	16%	1%	**21498**
	Canon Fronsac	100%	-	-	50%	35%	15%	**396**
	Côtes de Bourg	48%	52%	-	48%	40%	12%	**7005**
	Fronsac	100%	-	-	51%	37%	12%	**1311**
	Premières Côtes de Blaye ; Côtes de Blaye	53%	47%	-	51%	46%	3%	**17111**

[a] : the figures are given in percent of the total area of each appellation of origin

Table 5: Comparison of pyranometer and high-resolution spatialized irradiation mean daily data at the weather station of Villenave d'Ornon (44.789°N ; 0.577°E).G_{dp} = pyranometers mean daily values ; Bias = mean error (spatialized - pyranometer), RMSD = Root Mean Squared Difference ; Min. = the minimum daily difference, Max = the maximum daily difference ; N = the number of observations. The values between parentheses indicate the statistical indicator in fraction of the pyranometer values (G_{dp}). Except for N, the values are given in MJ m^{-2}.

Period	G_{dh}	Bias		RMSD		Min.	Max.	N
January	4.6	-0.5	(-9.9%)	1.0	(22.5%)	-3.3	1.8	155
February	7.7	-1.4	(-18%)	2.0	(25.8%)	-5.2	3.0	141
March	12.4	-1.8	(-14.2%)	2.4	(19.7%)	-7.4	1.3	155
April	16.4	-1.9	(-11.6%)	3.0	(18.3%)	-8.7	8.6	150
May	20.5	-2.7	(-13%)	4.0	(19.5%)	-10.8	9.3	155
June	23.3	-1.8	(-7.7%)	3.1	(13.1%)	-11.0	5.2	150
July	22.2	-2.2	(-9.9%)	3.7	(16.6%)	-10.8	5.3	155
August	19.6	-1.7	(-8.8%)	3.1	(16%)	-10.4	4.5	155
September	15.3	-1.7	(-11.2%)	2.7	(17.3%)	-10.4	6.1	150
October	9.3	-1.9	(-20.9%)	2.5	(27.4%)	-9.4	2.1	155
November	5.6	-0.3	(-5.8%)	1.3	(22.5%)	-3.4	3.5	150
December	4.1	-0.1	(-1.8%)	1.0	(25%)	-3.7	2.6	155
Year	13.4	-1.5	(-11.1%)	2.7	(19.8%)	-11.0	9.3	1826
Aug. – Sept.	17.5	-1.7	(-9.8%)	2.9	(16.6%)	-10.4	6.1	305

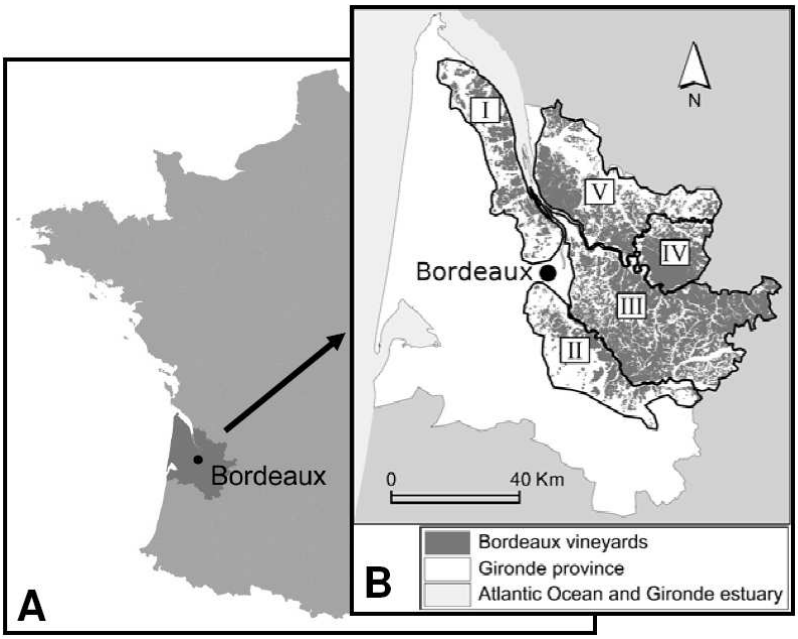

Figure 1: Maps of the study area. A: France, with the Gironde province and the city of Bordeaux. B: The Bordeaux winegrowing area, located in Gironde province. Figures in roman numbers indicate the number of the 5 sub-regions of Bordeaux winegrowing area (see table 1 for the list of the appellation of origin located in each region).

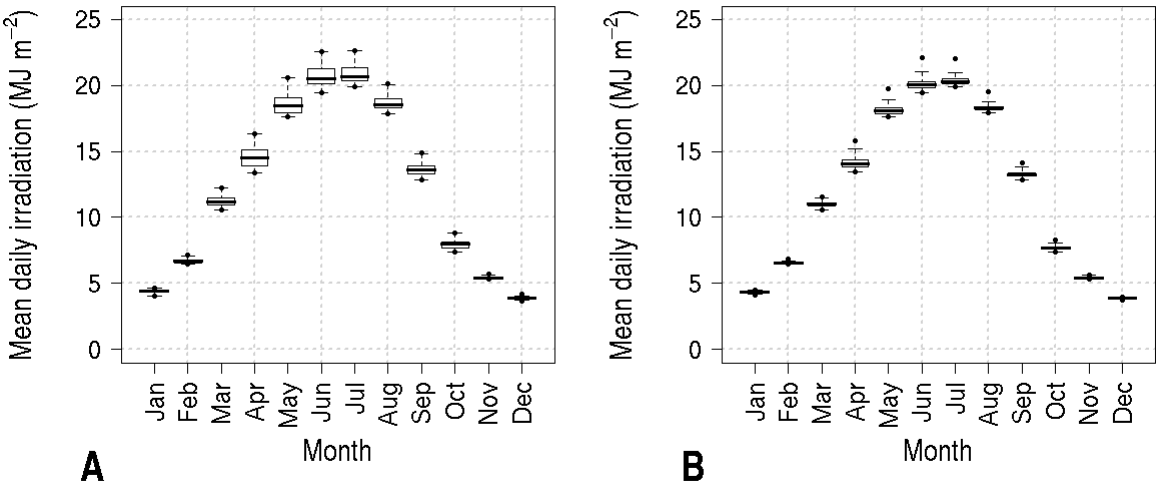

Figure 2: Box-plots of monthly means of daily irradiations, during the period 1986-2005, for Gironde province (A) and Bordeaux winegrowing area (B). Data used to elaborate each box are the mean daily irradiation values of each 500 m pixel. Points outside the boxes represent the minimum and the maximum values observed within each area.

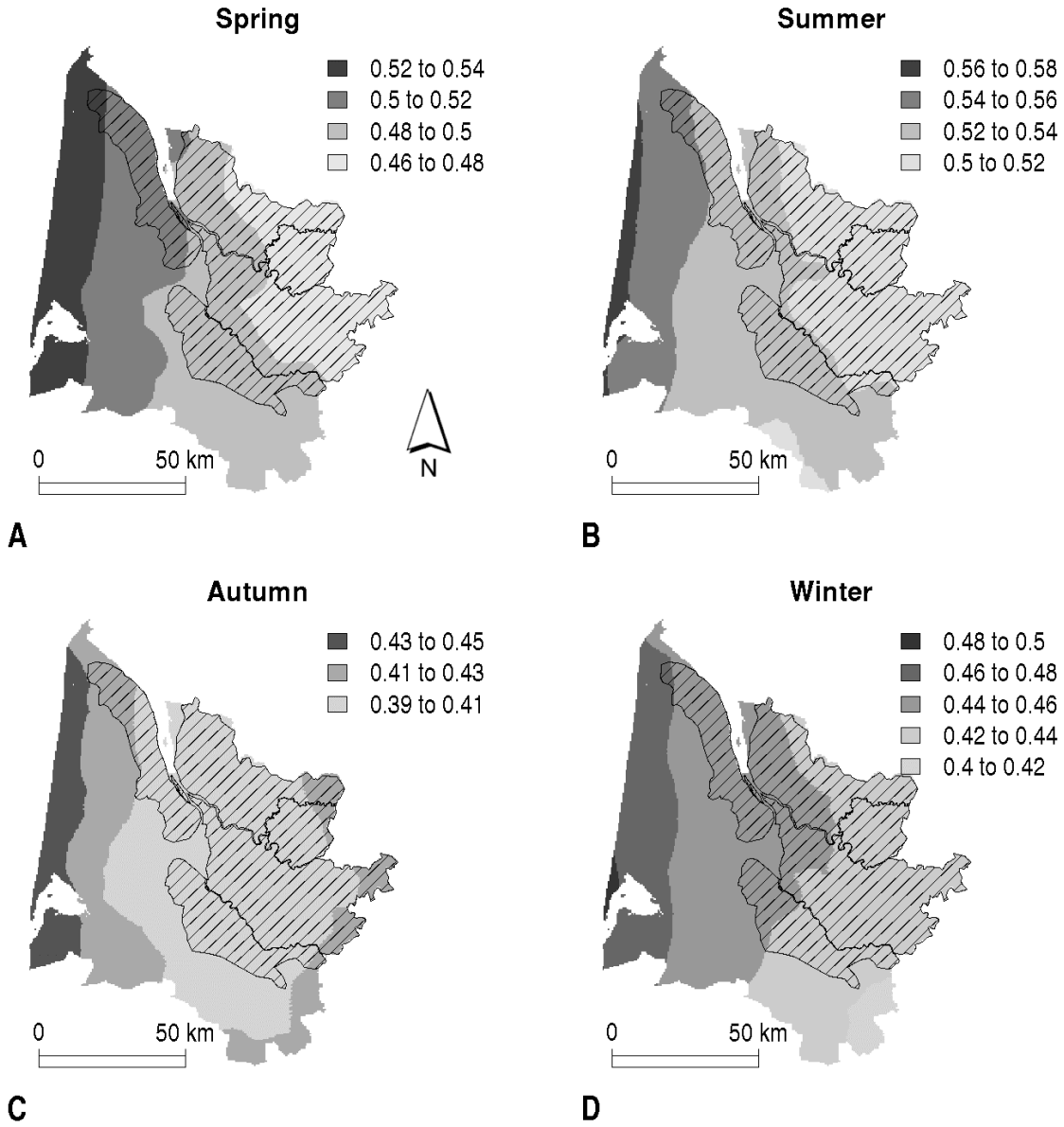

Figure 3: Seasonal maps of clearness index of Gironde province (period 1986-2005). The dashed areas represent the 5 sub-regions of Bordeaux winegrowing area (see figure 2B). A: “spring”, from April to June ; B: “Summer”, from July to September ; C: “Autumn”, from October to December ; D: “Winter”, from January to March.

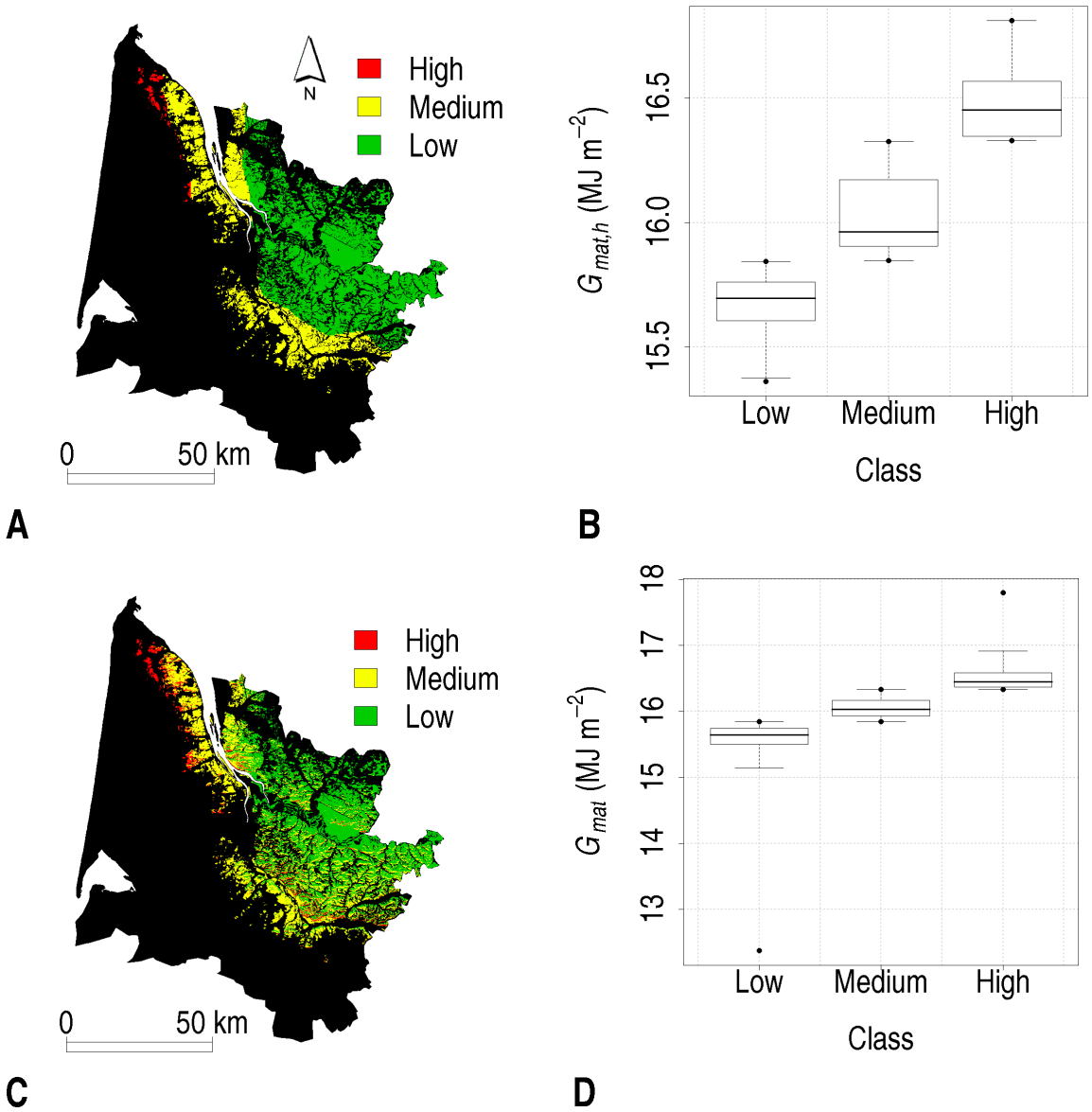

Figure 4: Zoning of Bordeaux winegrowing area based on the mean daily solar irradiation value from August to September ($G_{mat,h}$), for the period 1986-2005. A: map of $G_{mat,h}$ classes (horizontal surface zoning); B: box-plot of $G_{mat,h}$ values of the three classes ; C: map of G_{mat} classes (inclined surface zoning) ; D: box-plot of G_{mat} values of the three classes. Points on box-plots figures correspond to the extremes values of each class.

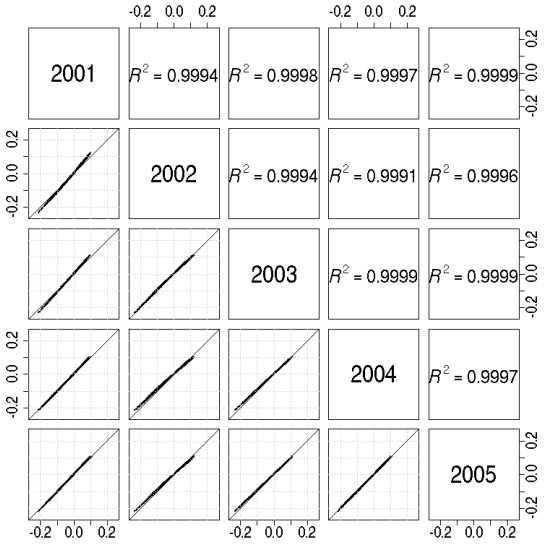

Figure 5: Scatter plot comparing, for different years, the values of the relative differences between G_{mat} on horizontal and inclined solar radiation data, of each pixel located in the Bordeaux winegrowing area (N = 948239).

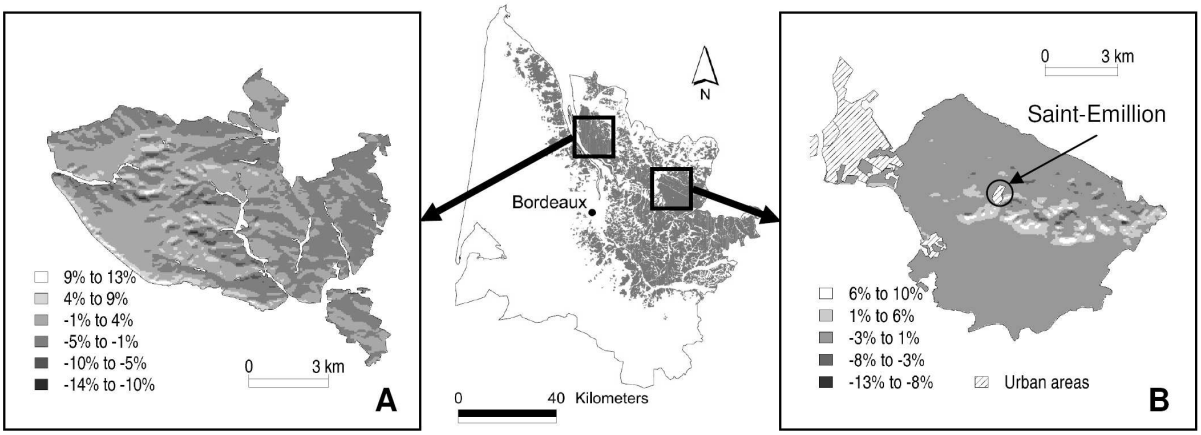

Figure 6: Mean daily solar irradiation data from August to September, for the period 1986-2005, of two appellations of origin (A.O.C.) areas of Bordeaux. The data is expressed in percent of the mean value of each whole area. A: A.O.C. Côtes-de-Bourg, B: A.O.C. Saint-Emilion (the circle indicates the localization of Saint-Emilion village.